Copy 260
RM E51A26

NACA RM E51A26
E 51 A 26

TECH LIBRARY KAFB, NM
0143644

NACA

RESEARCH MEMORANDUM

PRELIMINARY INVESTIGATION OF EFFECTIVENESS OF BASE BLEED IN REDUCING DRAG OF BLUNT-BASE BODIES IN SUPERSONIC STREAM

By Edgar M. Cortright, Jr. and Albert H. Schroeder

Lewis Flight Propulsion Laboratory
Cleveland, Ohio

CLASSIFIED DOCUMENT

This material contains information affecting the National Defense of the United States within the meaning of the Espionage Act, USC 50:31 and 32. Its transmission or the revelation of its contents in any manner to an unauthorized person is prohibited by law.

Information so classified may be imparted only to persons in the military and naval services of the United States, appropriate civilian officers and employees of the Federal Government who have a legitimate interest therein, and to United States citizens of known loyalty and discretion who of necessity must be informed thereof.

NATIONAL ADVISORY COMMITTEE
FOR AERONAUTICS

WASHINGTON
March 9, 1951

319.98/13

Classification cancelled (or changed to Unclassified)

By Authority of NSA Tech Pub Announcement #96
(OFFICER AUTHORIZED TO CHANGE)

By ..... Nov 56

.....
GRADE OF OFFICER MAKING CHANGE)

7 Feb 61
DATE

TECH LIBRARY KAFB, NM
0143644

2099

NATIONAL ADVISORY COMMITTEE FOR AERONAUTICS

RESEARCH MEMORANDUM

PRELIMINARY INVESTIGATION OF EFFECTIVENESS OF BASE BLEED IN REDUCING DRAG OF BLUNT-BASE BODIES IN SUPERSONIC STREAM

By Edgar M. Cortright, Jr. and Albert H. Schroeder

SUMMARY

The drag-reducing effectiveness of bleeding air to the base region of blunt-base bodies in a supersonic stream was investigated at a Mach number of 1.91. The first phase of the study consisted of base-pressure measurements on bodies of revolution with both a cylindrical afterbody and with conical boattails. In this phase, variable base bleed was provided from an external air supply. Base bleed was shown to be an effective means of reducing the base pressure drag. Increases in base-pressure coefficient of 0.04 were obtained with the cylindrical-afterbody configuration. The variation of base pressure with quantity of base bleed was such that bleed-air sources at ambient pressure or less could be utilized effectively.

The second phase of the investigation employed force measurements to determine whether drag reductions could be obtained under practical conditions of bleed air intake. Simple drilled holes in the cylindrical portion of a hollow cone-cylinder body of revolution with open base resulted in total drag coefficient reductions of 0.03. Bleed air intake through the nose resulted in only slight net-drag reductions.

INTRODUCTION

When bodies with blunt bases are submerged in a supersonic stream, the external air flow separates from the bodies at the bases. This separation results in a semidead air region at the base that is generally at a lower pressure than the ambient fluid. The

4770

resulting pressure drag of the surface area wetted by this semidead air is commonly referred to as "base drag."

With respect to total drag, base drag may assume varying degrees of importance depending on the particular body configurations under consideration. For bodies of revolution with cylindrical afterbodies and for extreme cases of the so-called blunt-trailing-edge airfoil, the base drag may be as much as 80 percent of the total-pressure drag at a Mach number of 1.9. Many other examples exist in which base drag is sufficiently large to be worthy of serious attention.

The results of a preliminary study of a technique designed to reduce the base drag of blunt-base bodies in a supersonic stream are presented herein. This technique consists in bleeding relatively small amounts of air into the semidead air region at the base and is hereinafter referred to as "base bleed." The experiments, which were conducted at the NACA Lewis laboratory in the summer and fall of 1950, consisted primarily of two phases. In the first phase, the variation of base pressure with base bleed was determined for a body of revolution mounting various boattail configurations and supplied with bleed air from a source independent of the model. In the second phase, drag measurements were made on a cone-cylinder body utilizing various means of bleed-air intake and ejection to determine whether drag reductions could be obtained under practical conditions of bleed-air intake. No attempt was made to study bleed systems in detail.

APPARATUS AND PROCEDURE

The investigation was conducted in the 18- by 18-inch (Mach number 1.91) supersonic wind tunnel at the Lewis laboratory. Test-section total temperature and pressure were approximately 150° F and atmospheric, respectively. The Reynolds number in the test section was approximately 3.2×10^6 per foot.

Pressure models. - The apparatus utilized to determine the variation of base pressure with amount of base bleed was primarily designed for a study of the pressure distributions over a series of conical boattails in the presence of a jet operating at pressure ratios up to 15. A sketch of the support and the models is shown in figure 1 and a photograph of the model assembly in the tunnel is shown in figure 2. (The boattail in the photograph is not one of those

2099

2099

included in the present report.) The model configurations were bodies of revolution made up of a single nose section with interchangeable half-bases to provide boattail variation. The nose and the half-bases were assembled with a support strut and splitter plate, resulting in an asymmetrical geometry at the rear of the body. Interference phenomena, however, were limited by the presence of the splitter plate to those associated with plate boundary layer and with small disturbances from the plate leading edge, which was swept back at an angle of 40°. The angle of attack was varied in the plane of the splitter plate. Bleed air was ducted into the model through the hollow strut and then was turned and passed through a screen before discharge from a convergent nozzle of exit diameter equal to one-half the maximum body diameter.

The assembled body of revolution had a fineness ratio of 12. The first half of the body was contoured according to equation (14) of reference 1, whereas the remainder was cylindrical except as modified by the presence of the conical boattails. Particular boattail geometries included in the investigation, along with the base-pressure instrumentation, are shown in figures 1(b) and 1(c). These models also included pressure instrumentation ahead of the base, which enabled the disturbance of the splitter plate to be qualitatively assayed. A pitot tube rake was provided at the nozzle entrance to determine the jet total pressure. Because earlier experiments had established a uniform flow at the nozzle entrance, a single tube of this rake was connected for the base-bleed investigation to a dibutylphthalate manometer board referenced to vacuum. This manometer was used for all pressure measurements. All static orifice diameters were 0.015 inch.

With the pressure models, the procedure consisted in merely recording the pressure distribution over the entire boattail with jet flow ranging from zero up to that corresponding to a jet pressure ratio of as much as 15. Only the data from the low range of jet pressure ratios are presented herein. Because only one quadrant of the base was instrumented, it was necessary to vary the angle of attack in both the positive and negative directions to get a representative base-pressure coverage at the angles of attack of 3° and 6°. In the case of the cylindrical-base model, a fairly complete survey was made of the variation of base pressure with jet pressure ratio, whereas for the boattailed bodies the general procedure was to determine the base pressure with no base bleed, the maximum base pressure, and the minimum base pressure with an occasional extra point to aid in fairing the data. Tunnel static pressure in the region of the boattail was determined by a calibration relating it to two side-wall static pressures. The dew

point was maintained within the range of -10° to 3° F. Pressure ratio was both increased and decreased to establish the absence of hysteresis in the variations.

2602

Force model. - A sketch of the force model, support system, and various model modifications is shown in figure 3. The basic configuration consisted of a hollow 20° cone-cylinder of fineness ratio equal to 8.8. From practical considerations, the nose was blunted to a 1/16-inch-diameter flat. The model was supported from the top of the tunnel by a shielded strut mounting strain gages in a moment-measuring circuit that was statically calibrated. Use of this system for drag determination assumed no pitching moment of the model about the support point. The fact that this assumption was obviously untrue because of the presence of the strut shield is referred to later in the section "Discussion of Results."

Three types of bleed-air intake were investigated at an angle of attack of 0. Type A consisted of drilled holes of progressively larger diameter in the nose of the model. Type B consisted of drilled 1/16-inch-diameter holes of progressively larger numbers starting from 1/4-inch downstream of the juncture of the cone and the cylinder. Holes were not located where the support shield covered region B. A typical type-B configuration is shown mounted in the tunnel in figure 4. Type C consisted of drilled 1/16-inch-diameter holes of progressively larger numbers starting from 1/2 inch upstream of the base. With each intake system was utilized a series of base configurations, D of figure 3, which varied the exit area A_b and area distribution in a systematic manner. In addition to the preceding configurations, two special models were investigated that consisted of the basic model with a hollow tube attached to the base by a perforated annular plate (E of fig. 3). A tube of $\frac{1}{2}$-inch diameter, $2\frac{1}{2}$-inches long and a tube of $\frac{7}{8}$-inch diameter, 3 inches long were utilized. Force measurements were made with the tubes wide open and capped.

Tunnel static pressure in the region of the model was determined from a calibration relating it to the upstream bellmouth total pressure, which was measured with four pitot tubes. Tunnel dew point was maintained in the same range as for the pressure-model tests.

2099

DISCUSSION OF RESULTS

The drag-reducing effectiveness of base bleed as obtained with the pressure models and as obtained with the force models are considered separately in the following discussion.

Pressure studies. - The results of the investigation of the variation of base pressure with base bleed are presented in figures 5 and 6 where base-pressure coefficient $C_{p,b}$ is plotted against jet pressure ratio P_j/p_0 for each of the body configurations at angles of attack α of 0°, 3°, and 6°.

$$C_{p,b} = \frac{p_b - p_0}{q_0}$$

where p refers to static pressure, q refers to dynamic pressure, and the subscripts 0 and b refer to free stream and base, respectively. Jet pressure ratio P_j/p_0, where P_j is the total pressure of the bleed air, is indicative of the bleed flow and is used only for convenience. The lowest recorded value of P_j/p_0 corresponds to no base bleed.

In the case of the cylindrical base model (fig. 5), the variation of base-pressure coefficient with radial distance from the body axis was small, hence an average value is plotted for each value of angular location θ, where θ is measured from the windward surface of the model. A mean curve has been faired through the data points for each angle of attack. From these curves it is seen that the base-pressure coefficient increases rapidly with slight increases in jet pressure ratio (or bleed flow). The maximum increase in base-pressure coefficient, approximately 0.04, appears to be independent of angle of attack. For all angles of attack, the minimum base drag was obtained with approximately the same jet pressure ratio of 0.86, which indicates that bleeding from free-stream static pressure or less should be effective. Also, because the base pressure decreased with increasing angle of attack and the bleed total pressure for minimum base-pressure drag remained the same, the required amount of base bleed increased slightly with angle of attack. Increasing the bleed flow beyond that required for minimum base-pressure drag caused the base pressure to decrease below its original value. This reversal of variation may be qualitatively explained in at least two ways. Entrainment of air from the annular semidead air region by the bleed air itself could cause a lowering of the base pressure with increasing jet velocities. In addition, the displacement effect of the jet may act in a manner

analogous to a support sting and thus cause the base pressure to approach the lower two-dimensional value with increasing jet pressure ratio and resulting displacement (see reference 2). Either explanation indicates that the ratio of jet-exit diameter to base diameter may be expected to have an effect on the variation of base pressure with jet pressure ratio.

The data obtained from the bodies with conical boattails with half-angle ϵ of 5.63°, 7.03°, and 9.33° and with a base-to-body diameter ratio of 0.704 are similarly presented in figure 6. For the boattail configurations, however, all the recorded base pressures were averaged for a single reading at each setting. In general, the effect of bleed was similar to that observed with the cylindrical-base model. Certain differences can be noted, however. It was necessary to utilize a higher value of jet pressure ratio ($P_j/p_0 \approx 1$) to bleed sufficient air to reach the minimum pressure-drag condition. This increase was probably a result of the higher initial base pressures. For all the boattails at $\alpha = 0°$, the maximum increase in base-pressure coefficient due to bleed was approximately 0.05, which was larger than for the cylindrical-base model. In addition, this maximum increase in base-pressure coefficient increased with increasing angle of attack, reaching a value of approximately 0.072 for the three boattails at $\alpha = 6°$. The decreases in pressure drag due to bleed were approximately independent of boattail angle (fig. 6), which may have resulted in this case from the fact that base pressure with no bleed did not vary with boattail angle.

Some question remains as to the accuracy of the preceding results when applied to a complete body of revolution because of support-system interference. Pressure disturbances resulting from misalinement of the splitter plate with the free stream or from plate boundary-layer growth might be expected to alter the pressure distributions upstream of the base and hence the base pressure. Although the data are not presented herein, the pressures upstream of the base varied in accordance with exact potential-flow theory at an angle of attack of 0. The pressures were slightly higher, however, as might be expected from the presence of the boundary layer on the body. No large variation with circumferential station was noted. For these reasons pressure disturbances from the plate leading edge and boundary layer were felt to be small at an angle of attack of 0. Another form of interference results from the fact that the plate boundary layer provides a possible source of air influx into the base region, which may affect the base pressure. This possibility is qualitatively borne out by the fact that for no bleed air at an angle of attack of 0 the cylindrical-base model registered a base-pressure coefficient of -0.132, whereas other observers have recorded

2099

values from -0.15 to -0.16 (references 2 to 4). This discrepancy indicates the possibility of some effect of support interference on the variation of base pressure with base bleed. Additional investigation is required to check this point.

Force studies. - The basic model for the force tests was chosen for ease of manufacture and does not represent a low-drag configuration. For this reason, appreciable improvements in base drag do not represent large percentage improvements of the total drag in this case.

With a closed base (no bleed flow), any modifications of the type attempted herein to the basic body would probably result in a change in the drag coefficient. This change, however, is not necessarily considered significant in the present investigation inasmuch as no effort was made to control any such effect. Of prime interest herein is the change in drag coefficient between the modified case with no bleed and with base bleed. In this regard it should be noted that this change in drag coefficient due to base bleed is representative of more than the change in base pressure, which was considered in the pressure studies. Any reduction in axial velocity of the bleed air from intake to exit will constitute a momentum loss and will appear as a drag increase. This drag component should be small for small values of bleed mass flow, particularly when the bleed intake is in a region of low-energy boundary-layer air. In the case of air intake through the nose, however, the internal drag should be more serious. In addition to this effect, a local pressure drag is probably established at each drilled side-intake hole during bleed by excess air that is deflected in the vicinity of each hole. Effects of bleed-air intake on the external friction drag are probably small because schlieren photographs indicated turbulence over most of the cylindrical portion of the body for all configurations with and without bleed.

The results obtained with the force models are presented in figures 7 to 9 where the body drag coefficient C_D based on the maximum cross-sectional area of the body A_m is plotted against the appropriate intake-area ratio for the three systems of air intake utilizing various base configurations. Intake-area ratio is defined as the ratio of side or nose-intake area, A_s or A_n, respectively, to the maximum body cross-sectional area A_m.

The configuration utilizing air intake in the relatively low pressure region just downstream of the cone (side-front intake) is represented by the data of figure 7. In this figure, the variation of drag coefficient with intake-area ratio is presented for four base

configurations. Curves are faired through the "no-bleed" points corresponding to a closed base and the points obtained with the most effective base configuration, which was the configuration with the base completely open, $A_b/A_m = 0.84$. The maximum decrement in drag coefficient due to base bleed of approximately 0.0325 was obtained with the largest intake area attempted and was a net gain. The unusual variation of drag coefficient with intake-area ratio for the no-bleed condition is not fully understood but may be due to boundary-layer effects on the friction and base drag combined with the following limitation of the drag-measuring technique. Presence of the support strut might be expected to introduce a pitching moment that would make the absolute magnitude of the drag forces obtained somewhat in error. If this error remained constant, the results of the investigation can be considered relatively unaffected. In the case of the side-front intake, however, locating the intake holes in the vicinity of the support strut might have varied this pitching moment and hence the indicated drag in an unpredictable manner.

In the case of the side-rear intake, data for all the bases investigated are presented (fig. 8). The maximum decrement in drag coefficient due to base bleed was approximately 0.03 and was mostly a net gain when the intake-area ratio A_s/A_m was approximately 0.35. For larger intake-area ratios, the net gain was less inasmuch as the presence of the bleed holes appreciably increased the drag for the case of no-bleed flow. In this case, the base with a hole of half the body diameter was slightly superior to the completely open base. Despite this and some other exceptions, it was generally observed in all the force tests that with a fixed bleed-air-intake geometry the reduction in total drag coefficient due to base bleed increased with increasing open area in the base A_b.

Where the bleed-air intake is obtained through the nose (fig. 9), the data are somewhat more difficult to interpret. The drag coefficient with no bleed was observed to vary in the manner expected, increasing with increasing nose bluntness. When the base was opened wide, however, the drag coefficient decreased to only approximately 0.013 below its original value for low values of intake-area ratio. For larger intake-area ratios, the net improvement in drag coefficient became negligible. The increase in forecone pressure drag from the original condition due to truncating the cone is theoretically negligible for these cases during bleed. Because external-flow departure angles obtained from schlieren photographs indicate that the base drag did decrease in a manner comparable with the side-intake models, particularly in the case of the larger intake-area ratios, it appears that the absence of appreciable net gain was primarily a result of high internal drag.

2099

The results of the side-intake tests are summarized in figure 10 where the increment in drag coefficient due to base bleed is plotted against intake-area ratio for the cases of the most effective bases investigated. Drag decrease due to base bleed is obtained quite rapidly and then appears to approach a limit, as would be expected. Utilization of side-front intake required more intake holes to obtain full benefit of base bleed because this intake region was at a lower pressure. The increments in drag coefficient of -0.03 are less than the -0.04 value predicted from the pressure investigation as a probable result of the aforementioned drag effects of handling the bleed air.

The purpose of the limited investigation of the basic body mounting hollow tubes supported by a perforated plate to the base was to attempt to stimulate increased reverse flow into the semidead air region by reaching downstream into the high-pressure wake. In order to evaluate the results, it was necessary to investigate the configurations with the tubes capped to determine if drag reduction might result from the presence of the tube alone. The results are summarized in the following table:

Base-tube configuration		Total drag coefficient, C_D		
Length (in.)	Inside diameter (in.)	No tube	Tube capped	Tube open
$2\frac{1}{2}$	$\frac{7}{16}$	0.402	0.388	0.385
3	$\frac{3}{4}$	.402	.394	.382

As shown in the table, there is a drag-reducing effect of the capped tubes alone. When the tubes were opened so as to permit air circulation the drag was further markedly decreased only in the case of the 3/4-inch inside-diameter configuration.

Typical schlieren photographs that illustrate the effect of base bleed on the base pressure as indicated by the external-flow departure angle are presented in figure 11. The flow over a conical boattail of half angle $\epsilon = 5.63^\circ$ is shown in figure 11(a). The departure angle markedly decreased when the amount of base bleed was set at the optimum value. The same effect of bleed is illustrated for the cylindrical-base force models in figures 11(b) and 11(c)

where a decrease in strength of the trailing shock waves with base bleed is also evident. All other models with bleed (including the nose-intake models) indicated qualitatively similar results. Estimates of the effect of base bleed calculated from the external-flow departure angles obtained from schlieren photographs correlate roughly with the pressure and force data.

2699

CONCLUDING REMARKS

Base bleed offers an effective means of reducing the drag of blunt-base bodies in a supersonic stream. Promising applications of this technique include blunt-base airfoils and blunt-base aircraft, missile, and projectile bodies. Such regions as the annular base around a nozzle exit, which may experience very low pressures because of jet effect, should also be susceptible to drag reduction. In addition, supersonic compressors utilizing blunt trailing-edge blades offer a conceivable application.

Although various authors have hypothesized with some success simplified flow fields that permit the prediction of base pressure characteristics for a limited family of bodies of revolution in a supersonic stream (references 2, 5, and 6), the detailed flow processes are quite complex and remain imperfectly understood. Consideration of base bleed is an added complication. Additional research, both theoretical and experimental, is required to further an understanding of the phenomena.

SUMMARY OF RESULTS

From a wind-tunnel investigation at a Mach number of 1.91 to determine the effectiveness of base bleed in reducing the drag of blunt-base bodies, the following results were obtained:

1. Bleeding the proper amount of air into the base region of bodies of revolution resulted in a substantial increase in the base pressure. In the case of the cylindrical-base body, an increase in base-pressure coefficient of approximately 0.04 was obtained at angles of attack of 0°, 3°, and 6°. In the case of the bodies with conical boattails of half-angle 5.63°, 7.03° and 9.33° and with base-to-body diameter ratio of 0.704, an increase in base-pressure coefficient of approximately 0.05 was obtained at an angle of attack of 0°, increasing to 0.07 at an angle of attack of 6°.

2. Total-drag-coefficient reductions of approximately 0.03 were obtained from force tests of a body of revolution with cylindrical afterbody utilizing simple drilled holes in the cylindrical portion as a means of air intake. Nose air intake yielded little net-drag decrease as a probable result of internal drag.

3. With a fixed bleed-air intake geometry, the reduction in total drag coefficient due to base bleed generally increased with increasing open area in the base.

Lewis Flight Propulsion Laboratory,
National Advisory Committee for Aeronautics,
Cleveland, Ohio.

REFERENCES

1. Jones, Robert T.: Estimated Lift-Drag Ratios at Supersonic Speed. NACA TN 1350, 1947.

2. Chapman, Dean R.: An Analysis of Base Pressure at Supersonic Velocities and Comparison with Experiment. NACA TN 2137, 1950.

3. Kurzweg, H. H.: New Experimental Investigations on Base Pressure in the NOL Supersonic Wind Tunnels at Mach Numbers 1.2 to 4.24. NOL Memo. 10113, Naval Ord. Lab., Jan. 23, 1950.

4. Charters, A. C., and Turetsky, R. A.: Determination of Base Pressure from Free-Flight Data. Rep. No. 653, Ballistic Res. Labs., Aberdeen Proving Ground, March 30, 1948.

5. Cope, W. F.: The Effect of Reynolds Number on the Base Pressure of Projectiles. Eng. Div. 63-44, British Nat. Phys. Lab., Jan. 1945.

6. Gabeaud: Base Pressures at Supersonic Velocities. Jour. Aero. Sci., vol. 16, no. 10, Oct. 1949, p. 638.

2099

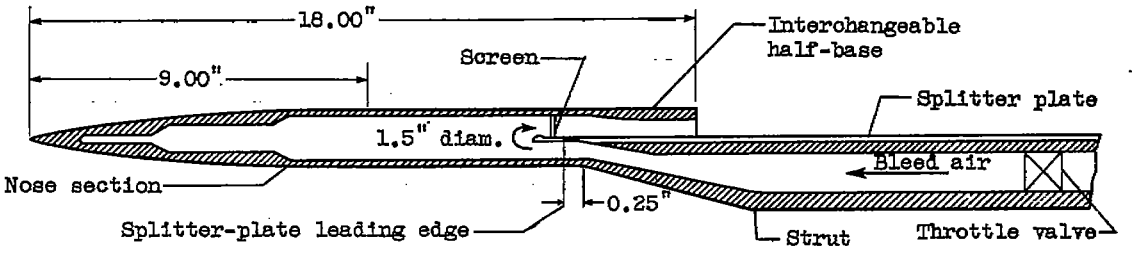

(a) Model and support with cylindrical-base configuration.

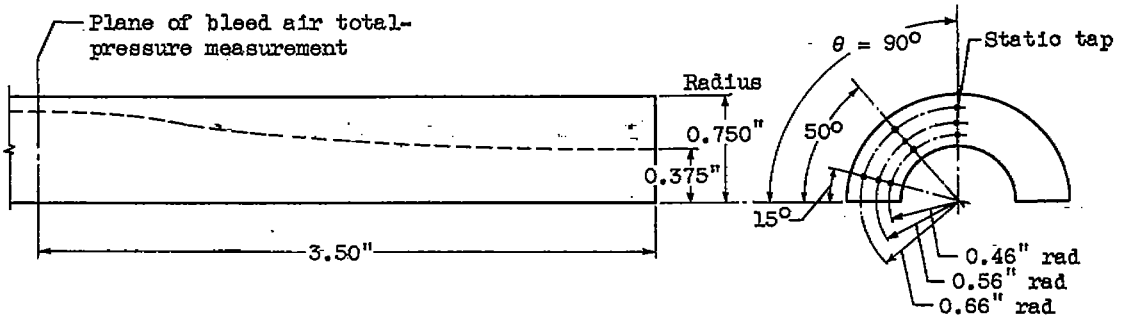

(b) Cylindrical-base configuration.

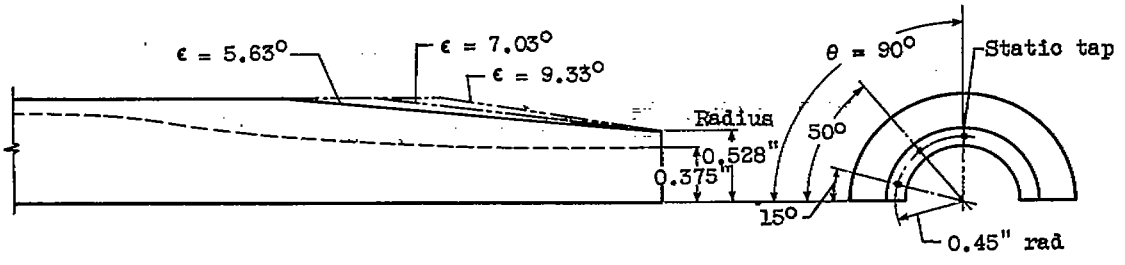

(c) Conical-base configuration.

Figure 1. - Sketch of pressure model, support strut, and various boattail configurations.

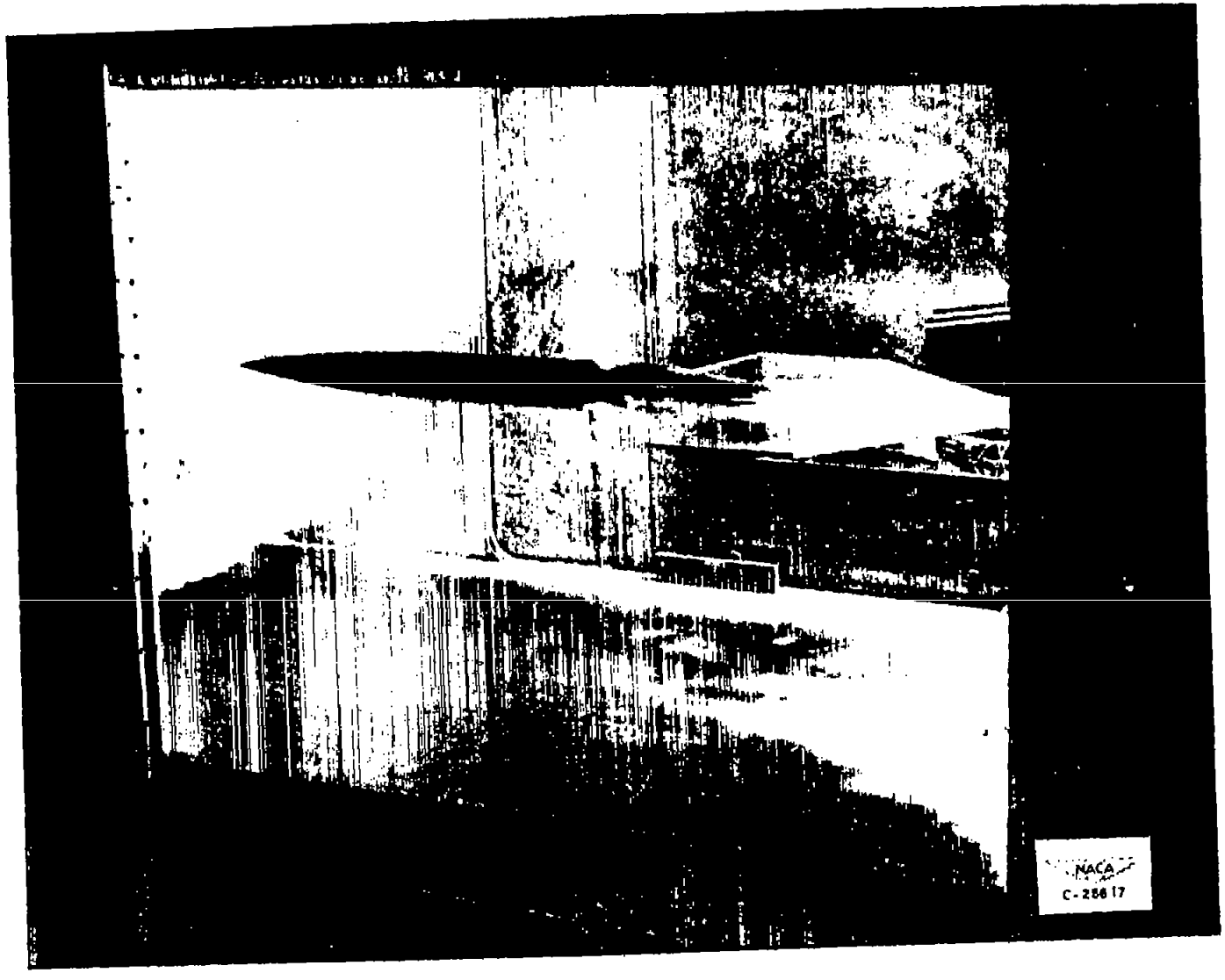

Figure 2. - Photograph of pressure model in 18- by 18-inch tunnel.

2099

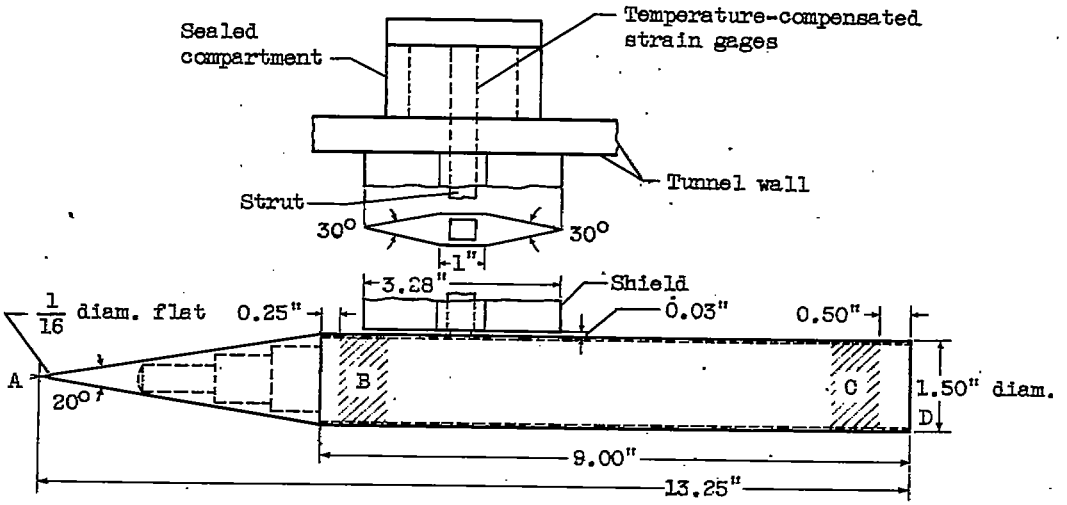

A Nose-intake-hole diameter: 3/32", 1/8", 5/32", and 3/16"
B Side-front intake region: 1/16"-diam. holes; 120, 206, 354, and 500 holes
C Side-rear intake region: 1/16"-diam. holes; 120, 180, 240, and 300 holes

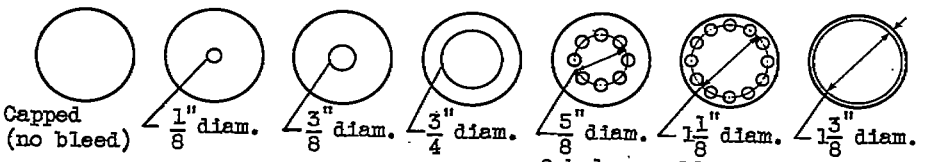

A_b/A_m	0	0.000695	0.0625	0.25	0.00556	0.00834	0.84
Base	1	2	3	4	5	6	7

D Base configurations: A_b, total open base area; A_m, body cross-sectional area

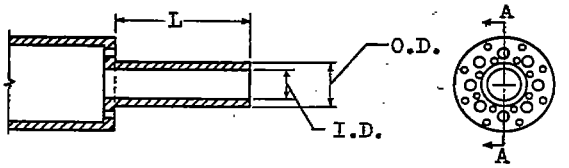

Section AA

Perforated annular plate of total open area A_p

Tube length L (in.)	I.D. (in.)	O.D. (in.)	A_p/A_m
$2\frac{1}{2}$	$\frac{7}{16}$	$\frac{1}{2}$	0.339
3	$\frac{21}{32}$	$\frac{3}{4}$	.318

E Special configurations

Figure 3. - Sketch of force model and balance system showing air-intake location and base configurations investigated.

22436

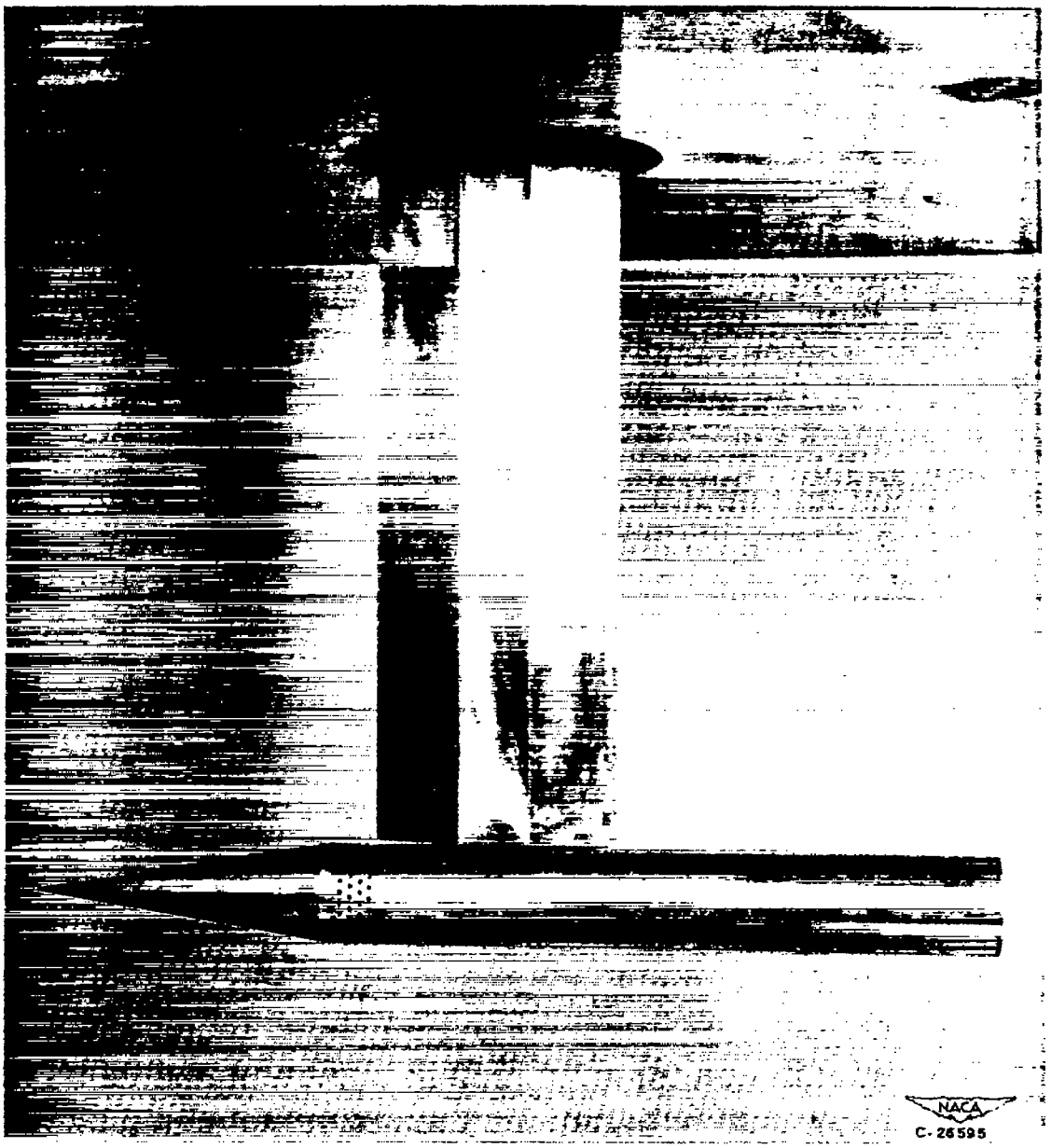

Figure 4. - Photograph of force model in 18- by 18-inch tunnel.

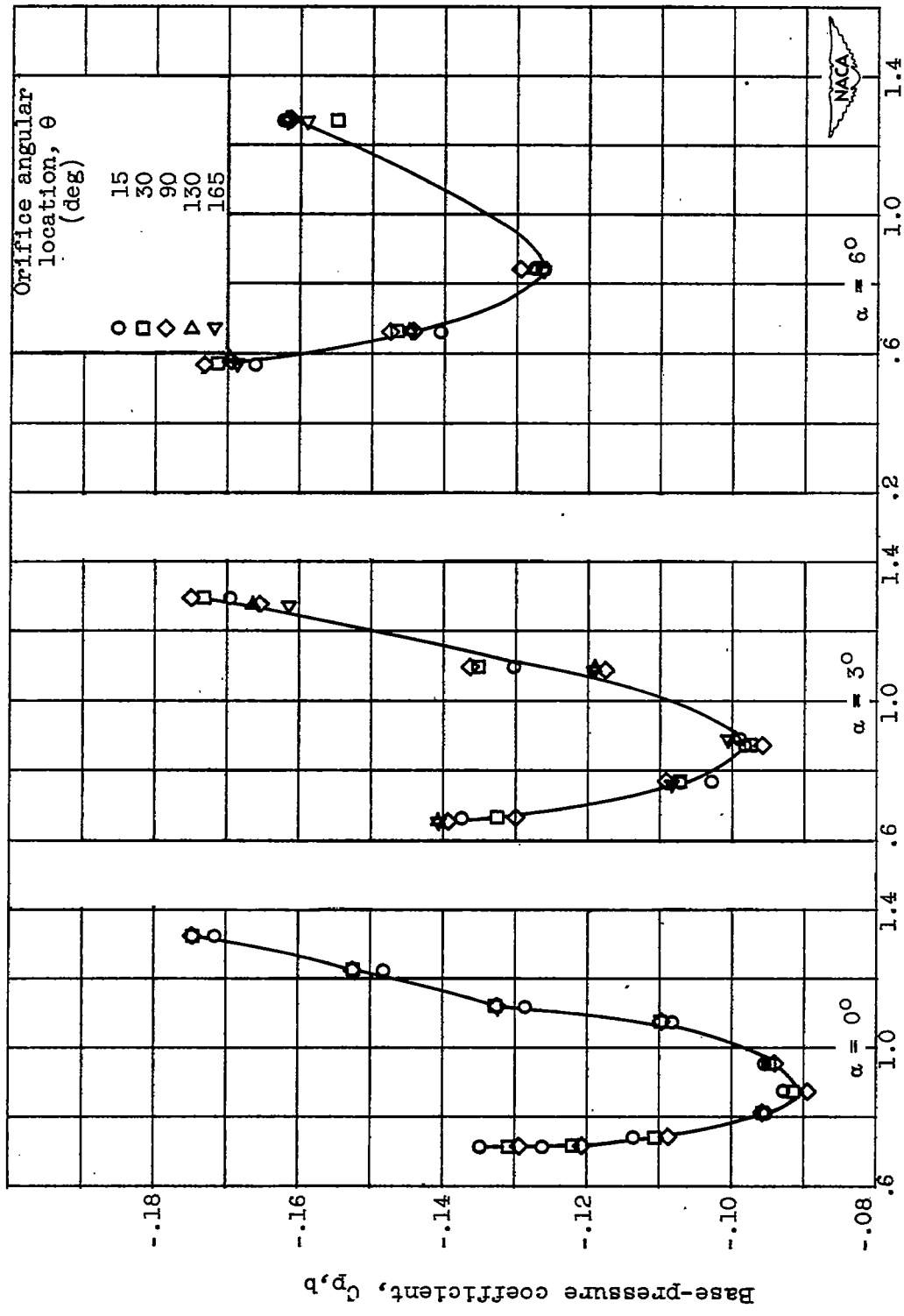

Figure 5. - Variation of base-pressure coefficient with jet pressure ratio for cylindrical-base model at angles of attack α of 0°, 3°, and 6°.

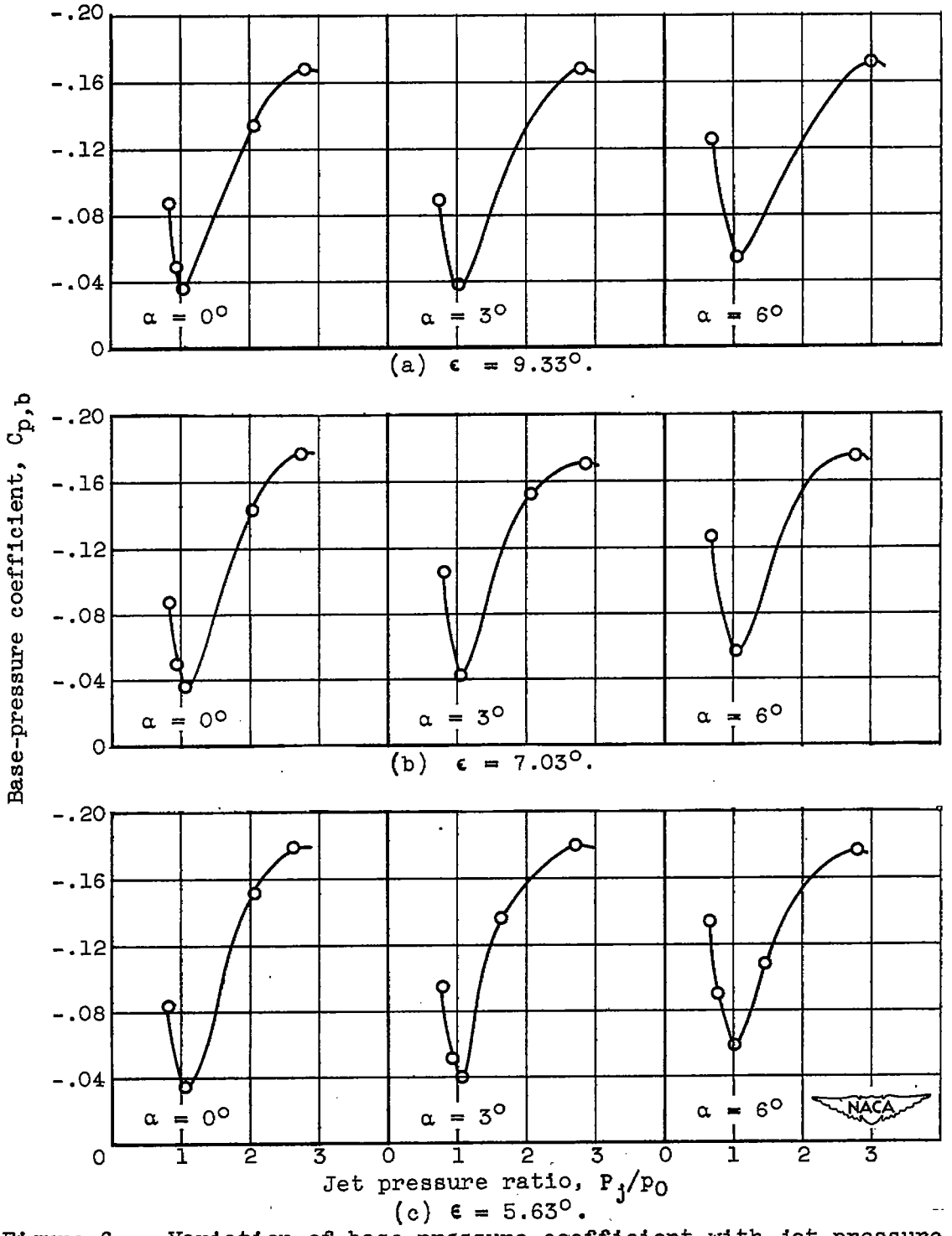

Figure 6. - Variation of base-pressure coefficient with jet pressure ratio for boattail configurations of half-angles ε equal to 5.63°, 7.03°, and 9.33° at angles of attack α of 0°, 3°, and 6°. Base-to-body diameter ratio, 0.704.

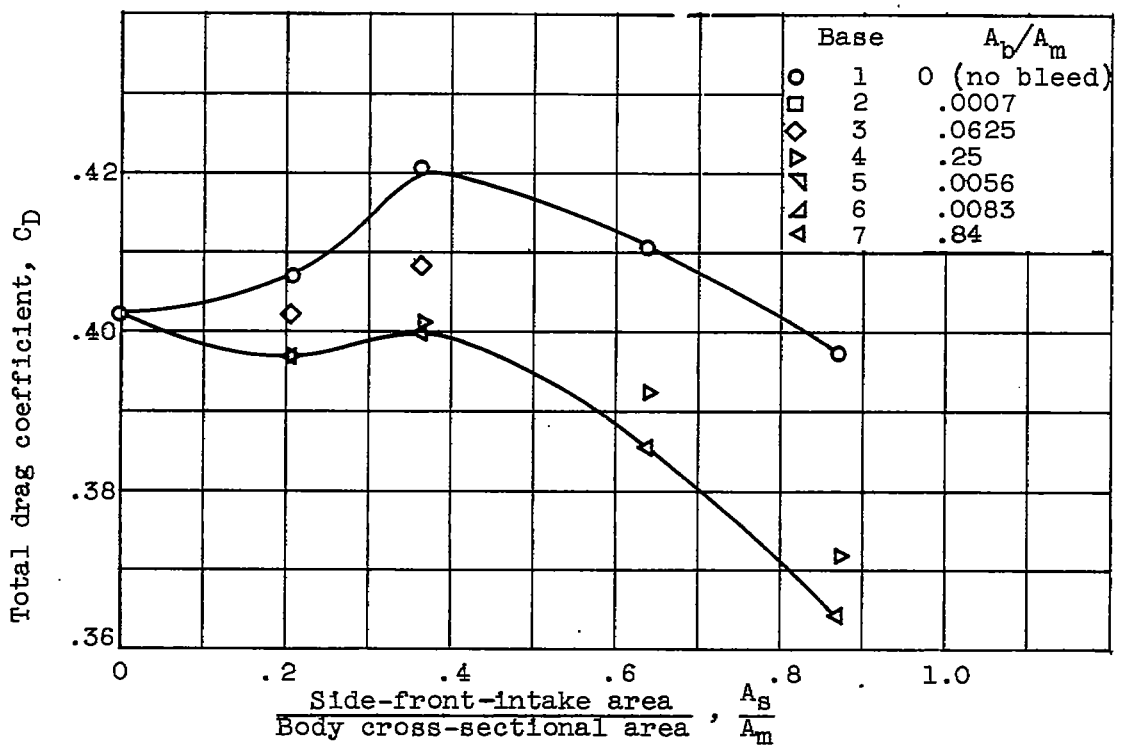

Figure 7. - Variation of total drag coefficient with side-front-intake-area ratio for various base configurations.

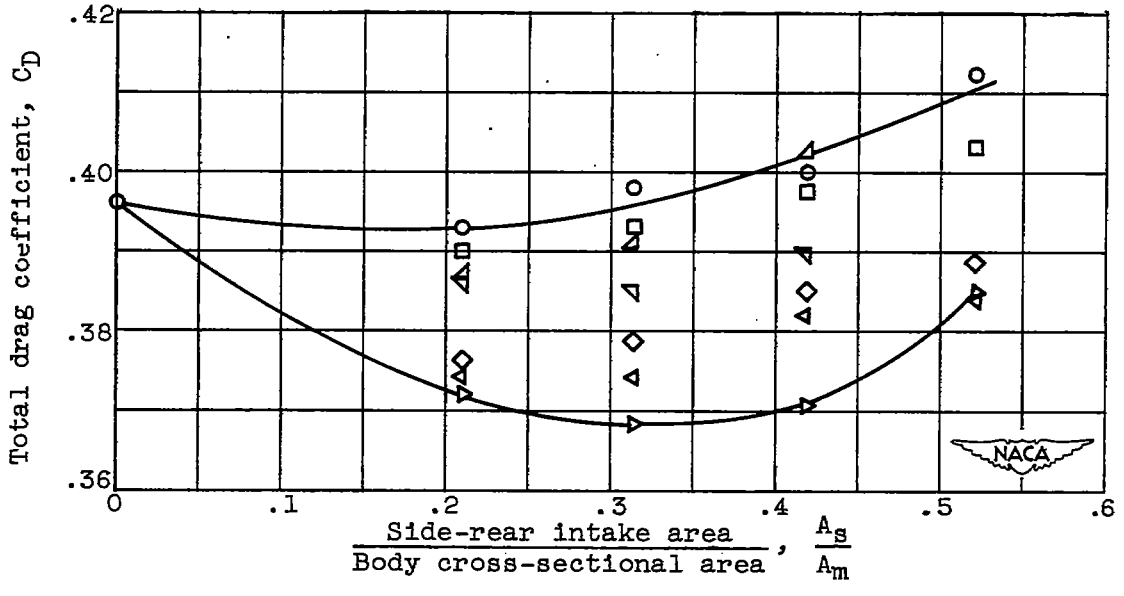

Figure 8. - Variation of total drag coefficient with side-rear-intake-area ratio for various base configurations.

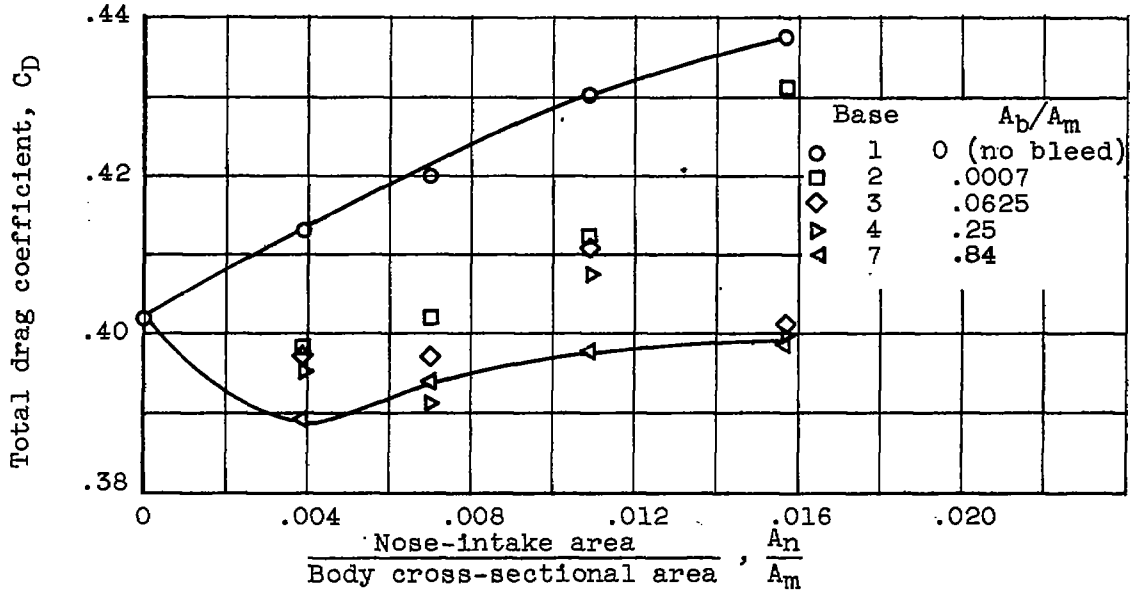

Figure 9. - Variation of total drag coefficient with nose-intake-area ratio for various base configurations.

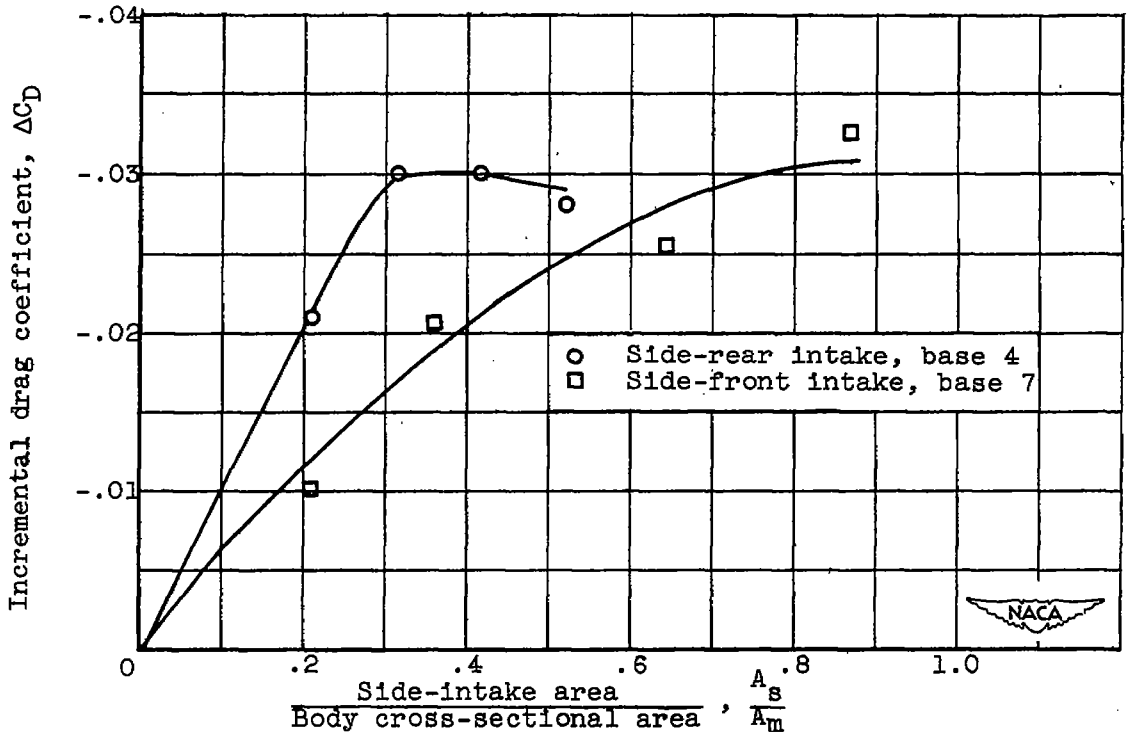

Figure 10. - Variation of incremental drag coefficient due to base bleed with side-intake-area ratio for cases of front and rear intake with best base configuration.

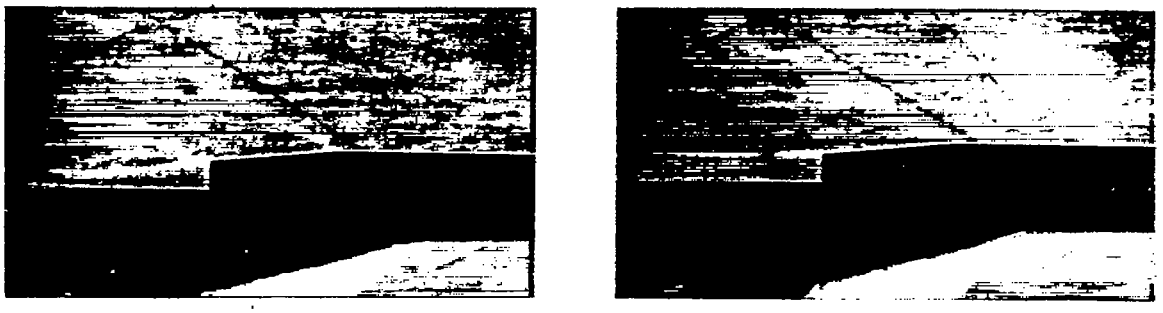

No bleed Base bleed; P_j/P_0, 1.08

(a) Pressure model; ϵ, 5.63°.

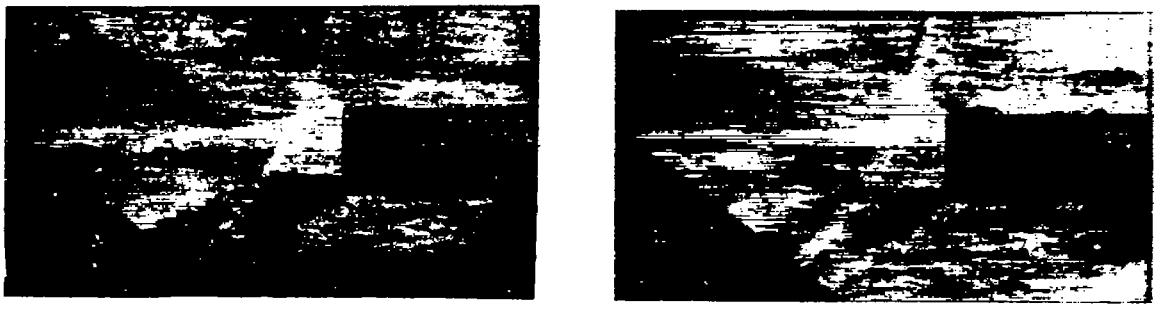

No bleed; base 1 Base bleed; base 7

(b) Force model-side rear intake; A_s/A_m, 0.31.

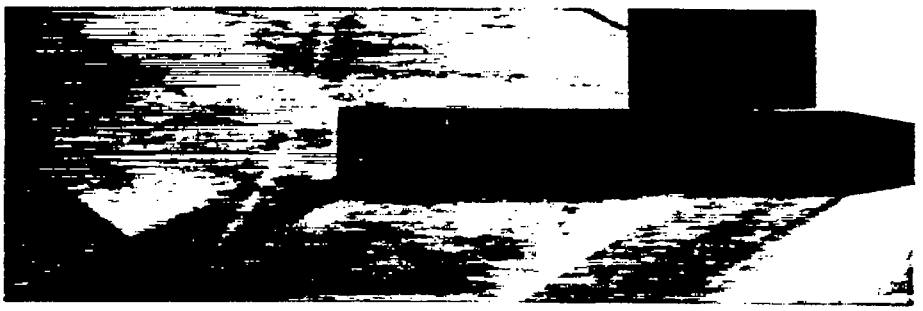

No bleed; base 1

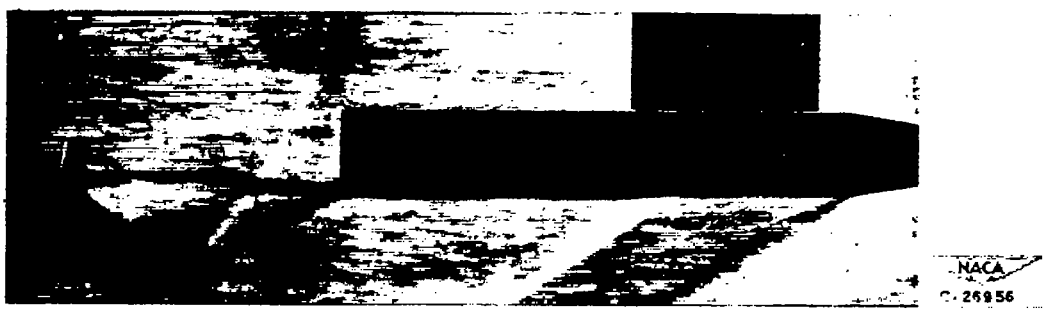

Base bleed; base 7

(c) Force model-side front intake; A_s/A_m, 0.87.

Figure 11. - Schlieren photographs of flow in base regions of typical pressure and force model configurations with and without base bleed at Mach number of 1.91.